

PACS numbers: 42.55.Px; 42.60.Lh; 42.25.Ja
DOI: 10.1070/QE2011v041n01ABEH014440

Stokes parameters of the radiation of transverse-single-mode InGaAs/AlGaAs lasers with a quantum-well active region

N.V. D'yachkov, A.P. Bogatov

***Abstract*. A study of lasers with two different heterostructures has revealed that the polarisation state of laser radiation depends strongly on the specific sample at pump currents corresponding to the regular behaviour of the light – current characteristic. Thus, the deviation of the radiation polarisation from linear can be used as a sensitive characteristic of the laser quality. It is found that anomalies in the power – current characteristic (the so-called kinks) are accompanied by a significant decrease in the degree of polarisation. The measured degrees of polarisation of spontaneous emission from samples (at pump currents much below the threshold) are in good agreement with the theoretical estimate obtained within the three-band model of optical transitions.**

Keywords: *semiconductor lasers, heterolaser, radiation polarisation, Stokes parameters.*

1. Introduction

Polarisation is one of the main characteristics of any radiation. However, the polarisation of radiation of semiconductor lasers has been little studied (possibly, because this characteristic is not so important for applications of these lasers).

Previous studies in this field were aimed at developing polarisation-insensitive semiconductor amplifiers [1, 2] or lasers with polarisation bistability [3, 4]; in this case, the only important condition was the dominance of one of the polarisation components. The later studies on the new types of semiconductor lasers (blue lasers [5], QD lasers [6], and vertical-cavity surface-emitting lasers (VCSELs) [7]) were similar in this respect.

There are grounds to believe that, being a fundamental characteristic of radiation, polarisation may contain information about the physical processes occurring in the laser cavity. Note that the polarisation of spontaneous radiation (emitted by a laser at pump currents much below the threshold) should primarily be affected by the material properties of the active region, whereas the laser radiation polarisation must be determined by the optical properties of the cavity. In this context, these polarisations can be considered as independent characteristics.

The simplest and most adequate model for calculating the material optical parameters of a quantum-well active region is the three-band model of optical transitions [8], which disregards band mixing. This model was used to calculate the dependence of the material gain and the additive to the real part of the active-region refractive index on the pump current. It was chosen to maximally reduce the number of fitting parameters without significant loss of reliability. In view of the good coincidence between the calculation results and experimental data, it was concluded in [8] that this model is optimal for the aforementioned purposes, because any complication may lead to not only cumbersome calculations but also to an unreasonable excess in the accuracy. In view of this, it is interesting to analyse the adequacy of description of the polarisation of spontaneous emission of a laser diode within the three-band model.

Concerning the polarisation of laser radiation, simultaneous generation of both (TE and TM) polarisation modes is out of the question because the gain of the quantum-well active region is significantly different for different polarisations. Hence, the presence of both polarisation components in laser radiation can only be caused by radiation scattering in the cavity. To determine its character, it is equally important to have information about the amplitude and phase relations between the polarisation components. It is well known that the Stokes parameters [9] may contain data of such kind on the radiation polarisation.

In view of the above considerations the main purposes of this study were, first, to analyse the possibility of using the three-band model to calculate the polarisation of spontaneous emission and, second, to establish a relationship between the polarisation of laser radiation and the specific features of laser diode cavity, which affect the basic characteristics. In addition, we estimated the informativeness of the Stokes parameters as independent characteristics of laser diodes.

2. Laser diodes and measurement technique

The objects of study were high-power transverse-single-mode lasers based on GaAs/AlGaAs and InGaAs/AlGaAs heterostructures with a quantum-well active region and a ridge optical waveguide [10, 11]. These devices were chosen because they are best studied, simple, and relatively stable. The lasers under study were divided into two groups: A and

N.V. D'yachkov, A.P. Bogatov P.N. Lebedev Physics Institute, Russian Academy of Sciences, Leninsky prosp. 53, Moscow, 119991 Russia; e-mail: bogatov@sci.lebedev ru

Received 27 September 2010
Kvantovaya Elektronika **41** (1) 20 – 25 (2011)
Translated by Yu.P. Sin'kov

B. The active-region material in the samples of group A, with a working wavelength of 0.85 μm, was unstrained GaAs, whereas the active region in the samples of group B (0.98 μm) was a strained InGaAs layer. The ridge widths in all lasers were very similar: 5.0 – 5.5 μm, and the active-region thicknesses ranged from 8 to 9 nm. The threshold currents and differential efficiencies of all lasers were in the ranges of 40 – 80 mA and 0.75 – 0.9 W A^{-1}, respectively.

The laser power supply was based on a combiner of two (dc and ac) signals, with an emitter follower at the output. The radiation intensity was measured by a conventionally connected FD-24k photodiode, biased by 8 V. The measurement system was calibrated using test power measurements by an OPHIR NOVA II meter with a 12A-P measurement head. The differential characteristics were measured by the technique similar to that described in [12], where an ac signal (~ 2 kHz) was applied at the corresponding input of the power supply, with subsequent detection of the alternating component of the radiation power and the voltage across the laser diode. The spectral measurements were performed using a DFS-24 spectrometer with a linear photodiode array instead of the exit slit. A similar scheme was described in [13]. The far-field pattern was recorded using a technique similar to that reported in [14].

The Stokes parameters were measured using two film polarisers, a phase plate, a Fresnel rhomb, and a photodetector. A simplified scheme of the setup for polarisation measurements is shown in Fig. 1. The analyser and plate were fixed in precision rotational attachments, which were brought into motion by computer-controlled stepper motors. The Fresnel rhomb was only used to measure the phase shift introduced by the phase plate and the position of its fast and slow axes. The polariser also served as an auxiliary tool to set the initial orientation of the plate. The polarisation data were reduced to the three Stokes parameters, S_1, S_2, and S_3, normalised to the total intensity (zero parameter). The coordinate axes were oriented so as to make the x axis lie in the plane of the layers. With these coordinate axes,

$$S_1 = \frac{I(0^\circ) - I(90^\circ)}{I}, \quad S_2 = \frac{I(45^\circ) - I(135^\circ)}{I}, \quad S_3 = \frac{I_R - I_L}{I}, \tag{1}$$

where $I(0^\circ)$, $I(90^\circ)$ are the intensities of the TE- and TM-polarised components, respectively; I is the total intensity; $I(45^\circ)$ and $I(135^\circ)$ are the intensities of the radiation passed through an analyser oriented at $\alpha = 45^\circ$ and 135° with respect to the x axis; and I_R, I_L are the intensities of the right- and left-hand circularly polarised components, respectively.

In our case the zero Stokes parameter is unity by definition, and zero angle α corresponds the analyser orientation at which $S_2 = 0$ for the spontaneous mode of the laser diode. Therefore, the degree of polarisation can be written as

$$P = (S_1^2 + S_2^2 + S_3^2)^{1/2}. \tag{2}$$

Our technique for measuring the Stokes parameters is similar to that described in [15].

Along with measurements of all reduced Stokes parameters for a discrete set of pump currents, we also performed a quasi-continuous measurement of S_1 in the entire range of pump currents for each laser by recording the quasi-continuous light – current characteristic of the laser + analyser system at two different analyser orientations, corresponding to the angles $\alpha = 0$ and 90°.

All lasers were investigated in the cw regime on a heatsink without thermostabilisation, at room temperature and pump currents up to 300 mA.

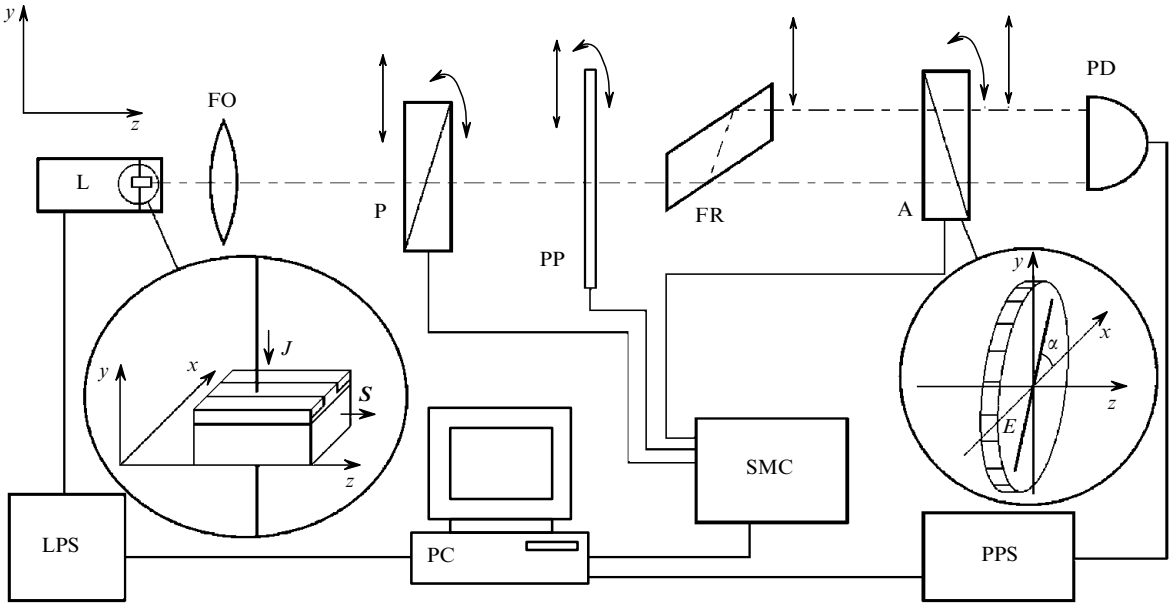

Figure 1. Schematic of the experimental setup for measuring Stokes parameters: (L) laser in a holder (***S*** is the normal to laser diode output face and J is the pump current direction), (LPS) digital laser power supply, (FO) focusing optics, (P) polariser, (PP) phase plate, (FR) Fresnel rhomb, (A) analyser (E is the analyser transmission axis), (PD) photodiode, (PPS) photodiode power supply, (SMC) stepper motor control, and (PC) personal computer with a built-in DAC – ADC unit.

3. Measurement results and discussion

As an illustration, we present the data for two samples: No. 1 (group B) and No. 2 (group A), which appear to be most typical. Figure 2 shows their light – current characteristics. The light – current characteristics of sample 1 [curve (*1*)] look most regular. At the same time, for some samples (from both A and B groups) these characteristics had an anomaly: a weakly pronounced kink at a lasing power above 100 mW. An example of such a light – current characteristic is curve (*2*) in Fig. 2. The physical nature of this anomaly is the optical nonlinearity related to hole burning. This effect leads to a change in the transverse (i.e., perpendicular to the resonator axis) profile of the effective refractive index in the plane of the layers (horizontal direction).

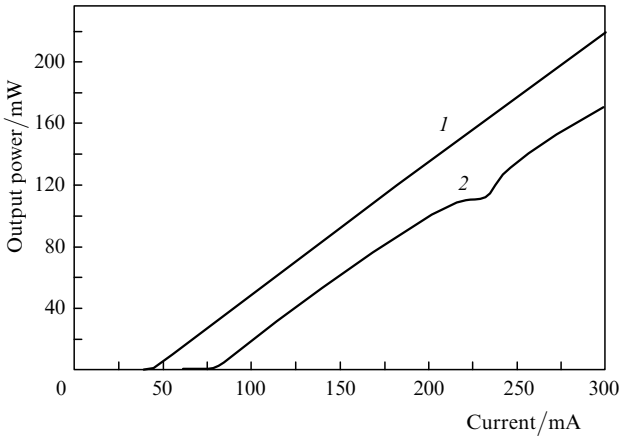

Figure 2. Light – current characteristics of samples (*1*) 1 and (*2*) 2.

These anomalies are most pronounced for lasers with a 'weak' horizontal waveguide (see, for example, [16, 17]). In our case the ridge laser design makes horizontal waveguide rather efficient. However, in some samples deviations from process parameters lead to deterioration of waveguide properties in particular region along the resonator axis, which causes anomalies in the light – current characteristic in the form of weakly pronounced kinks. The effect of this nonlinearity on the laser radiation characteristics was analysed in detail in [18].

Figure 3 shows the dependences of the Stokes parameters on the pump current for the aforementioned samples. The dependence of S_1 on the pump current can be divided into three ranges. These are two terminal ranges, $J \ll J_{th}$ (with dominance of spontaneous emission) and $J > J_{th}$ (with dominance of laser radiation), and an intermediate range for $J \lesssim J_{th}$, where amplified spontaneous emission makes a significant contribution to the total radiation intensity.

In the range $J \ll J_{th}$ the degree of polarisation is determined by the difference in the probabilities of spontaneous emission into the TE and TM modes. This value depends only on the squares of the corresponding matrix elements for interband transitions and band occupancies. Obviously, for the spontaneous emission in the bulk of active region without stresses, the spontaneous emission is natural polarised light, for which $P = 0$. In our case (Fig. 3), nonzero S_1 and, therefore, P are due to only the quantum-size effect and/or stress. An analysis showed that for the

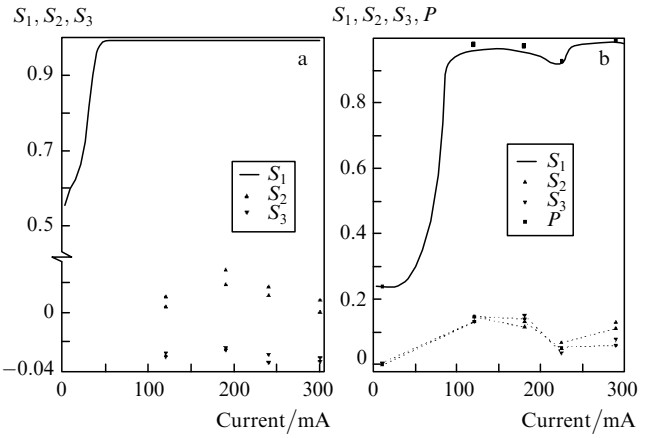

Figure 3. Dependences of the Stokes parameters on the pump current for samples (a) 1 and (b) 2. The part of the scale corresponding to S_2 and S_3 for sample 1 is enlarged.

samples of group A the S_1 values at the current $J \to 0$ are ~ 0.25, whereas for the samples of group B (with a strained active region) they amount to ~ 0.55. The parameters S_2 and S_3 have values close to zero (within the measurement accuracy) in this range.

Let us estimate the parameter S_1 at pump currents near the threshold transparency for TE-polarised radiation by expressing it in terms of the intensities W_{TE} and W_{TM} of the TE- and TM-polarisation components of spontaneous emission:

$$S_1 = \frac{W_{TE} - W_{TM}}{W_{TE} + W_{TM}}. \tag{3}$$

In turn, the intensity of spontaneous emission of specified polarisation is determined by the probabilities (per unit time) of different radiative transitions with emission of a photon of this polarisation, multiplied by the energies of these transitions E_{tr} (the probabilities for the emitted photon to enter the waveguide is assumed the same for both polarisations). In our case we can select two types of transitions: to the light- and heavy-hole subbands (lh and hh, respectively). The probabilities of emitting photons of different polarisations are related to the probabilities of these transitions through the polarisation factors $P_{c\sigma}^{TE,TM}$. As a result, we have

$$W_{TE,TM} \propto \sum_{\sigma=hh,lh} P_{c\sigma}^{TE,TM} \int_{Eg\sigma}^{\infty} R_{c\sigma}(E_{tr}) E_{tr} dE_{tr}. \tag{4}$$

The $P_{c\sigma}^{TE,TM}$ values are equal to the ratios of the squares of the corresponding matrix elements $|M_{cv}|^2$ to the $|M_{avg}|^2$ value, averaged over three polarisations [19]. In our case, they have the form

$$P_{chh}^{TE} = 1.5, \quad P_{clh}^{TE} = 0.5,$$
$$P_{chh}^{TM} = 0, \quad P_{clh}^{TM} = 2.0. \tag{5}$$

The $R_{c\sigma}(E_{tr})$ value is the integrand in formula (14) for the current density from [8]:

$$R_{c\sigma}(E_{tr}) \propto m_{red\,\sigma} E_{tr} f_c (1 - f_v). \tag{6}$$

The arguments of the Fermi distribution functions f_c and f_v in (6) for the carriers coincide with the corresponding arguments from [8]. The theory reported in [8] allows one to calculate (6) if we know the band gap E_g; the splitting of the top of the valence band into the light- and heavy-hole subbands, ΔE; the electron and hole effective masses in the quantum-well plane, m_c, m_{hh}, m_{lh}, the temperature T; the carrier concentration N; and the active-region width d. The carrier concentration will be assumed such as to equate the difference in the quasi-Fermi levels to E_g. In this case, the final result is independent of d.

Most of the necessary material parameters of the medium (effective masses of carriers and E_g) can be found in the tabular data on materials and heterostructures [20, 21]. The ΔE value was estimated based on the known data on the energy band diagram of the structure.

The specific values of the quantities necessary for calculations, the calculation results, and the comparative experimental data are listed in Table 1.

A comparison of the experimental and theoretical values of S_1 for spontaneous emission in the range $J \ll J_{th}$ indicates that the model chosen yields a fairly good result. Some underestimation (in comparison with the corresponding experimental data) of the S_1 values can be caused by the reabsorption of TM-polarised radiation in the cavity bulk, which is ignored in the model. Nevertheless, the average difference in the degrees of polarisation for different structures (~ 0.36) coincides (within the error) with the corresponding experimental value (~ 0.34). This fact confirms the adequacy of the model chosen to simulate the polarisation characteristics of the lasers.

In the intermediate range of currents ($J \lesssim J_{th}$), up to the lasing threshold, the parameter S_1 generally monotonically increases, as follows from the data in Fig. 3. Here, polarisation controls mainly the amplification (reabsorption) of spontaneous emission. Since this process is well known and was investigated by other methods (see, for example, [13]), its analysis is beyond the scope of this study.

In the other range of practical importance ($J > J_{th}$) the main contribution to the optical beam is from the lasing component (TE mode in our case). The investigations showed that in the lasing regime the polarisation behaves similarly for samples A and B. In the ideal case (the spontaneous emission is neglected and the layers of the laser structure are optically perfect), S_1 and, therefore, the degree of polarisation P must be equal to unity. One can see in Fig. 3 that the experimental value of the parameter S_1 differs from unity: it is in the range $0.5 < S_1 < 0.9995$ for different samples. The S_1 value for the radiation from the first sample in the lasing regime turned out to exceed the upper limit of the measurement range of the film polariser; however, the measured value of S_3 (~ 0.03) makes it possible to estimate S_1 from above: $S_1 \leqslant (1 - S_3^2)^{1/2} \approx 0.9995$.

When analysing the data in Fig. 3, one can also see that, beginning with some current, S_1 stops to increase and tends to a constant value. This fact indicates that the difference of S_1 from unity is not due to the presence of spontaneous emission component in the optical beam. Moreover, for the samples with anomalies in the light–current characteristic, S_1 drops in a narrow range of currents (near ~ 230 mA in the aforementioned case). This range almost coincides with the range where a kink occurs. This effect is also illustrated by the results obtained for other basic characteristics of the lasers (are presented in Figs 4–6). The fact that in this case the kink is due to the deformation of the transverse distribution of the laser mode field, is primarily evidenced by the comparative data in Fig. 4 for the samples with and without an anomaly in the light–current characteristics. According to the previous studies [12, 22], the laser radiation spectrum (Fig. 5b) and the differential resistance (Fig. 6) behave anomalously near the kink. In the lasers with a light–current characteristic without kinks, the directional patterns have the same shape (Fig. 4a). For example, the corresponding (normalised to maximum) curves for sample 1 coincide with an error not larger than $\sim 1\,\%$. The other characteristics of such lasers also behave regularly (Figs 5a, 6).

When analysing the entire set of experimental data, one can distinguish two mechanisms that are responsible for the polarisation characteristics of the laser beam. The first is responsible for the change in the polarisation state. This mechanism quantitatively dominates when

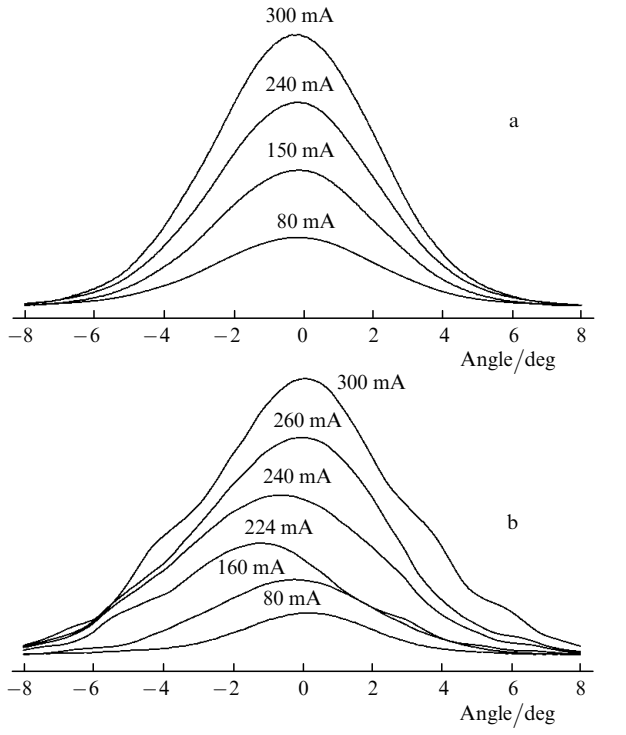

Figure 4. Horizontal directional radiation pattern at different pump currents for samples (a) 1 and (b) 2.

Table 1.

Sample type	m_c/m_0	m_{hh}/m_0	m_{lh}/m_0	E_g/eV	T/K	ΔE/meV	S_1	
							Calculation	Experiment
A	0.067	0.105	0.23	1.46	300	17–25	0.09–0.19	0.20–0.245
B	0.060	0.08	0.17	1.29	300	45–55	0.42–0.54	0.56–0.60

Note: m_0 is the electron mass.

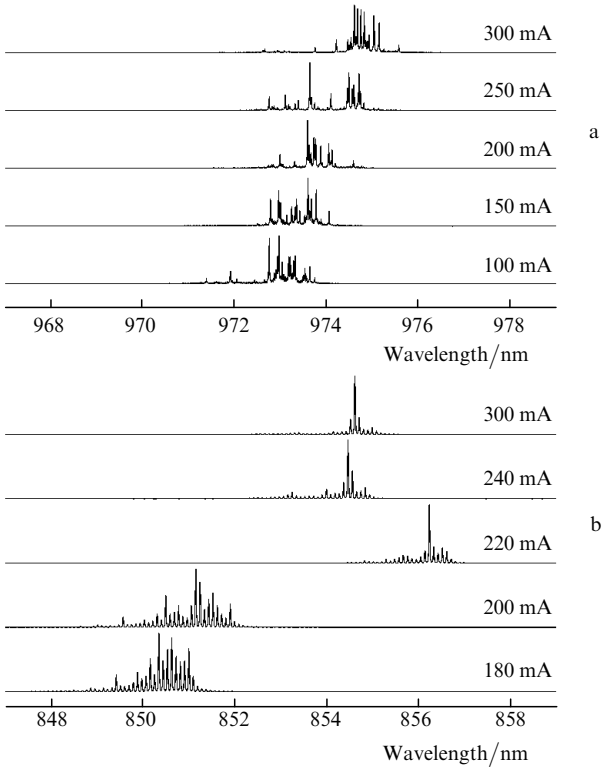

Figure 5. Radiation spectrum at different pump currents for samples (a) 1 and (b) 2.

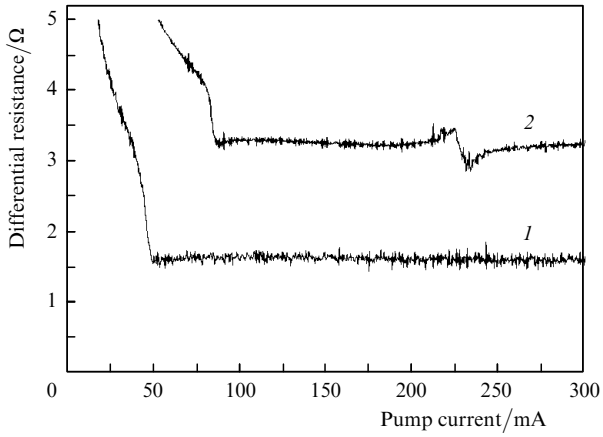

Figure 6. Dependences of the differential resistance of lasers on the pump current for samples (*1*) 1 and (*2*) 2.

$$1 - P \ll (S_2^2 + S_3^2)^{1/2}.$$

It is in essence coherent scattering of TE-polarised radiation with excitation of a TM wave of the same frequency and with a constant phase shift with respect to the TE wave. The TM wave induced by this process is coherent with the TE wave. Investigations showed that this mechanism is generally characteristic of lasers operating beyond the anomalies of the light–current characteristic and can be implemented, for example, due to the static optical inhomogeneities of the laser cavity medium, which exhibit birefringence. These static inhomogeneities can be caused by the irregularities of interfaces in the laser structure; 'frozen' stresses, which arise when the laser chip is soldered on the heatsink; stresses caused by the lattice mismatch between different layers of the heterostructure, including the active layer; and the differences between the crystalline properties of the metallised surface and the properties of the internal layers. There also may be stresses at the semiconductor–insulating layer interface, which can depend, in particular, on the ridge surface relief. These stresses are determined by the laser production technology; therefore, their pattern is different for different samples. In addition, stresses can be caused by temperature gradients in the laser cavity. In this case, the spatial distributions of these stresses and, correspondingly, the parameters S_2 and S_3 depend on the pump current. The calculation of possible stresses, the corresponding tensor of the additional component of permittivity, and the amplitude of the arising TM wave is beyond the scope of this study. Here, we will only state that the $(S_2^2 + S_3^2)^{1/2}$ value can be used as a quantitative characteristic of the quality of the cavity medium in a specific diode. For example, for the sample with the most regular light–current characteristic [Fig. 2, curve (*1*)], this value was below 0.03, whereas for some samples, which also demonstrated a relatively regular light–current characteristic at a high differential efficiency, it exceeded 0.5. Thus, the range where the optical quality of the cavity can be characterised obviously exceeds one order in magnitude.

The second mechanism of the formation of polarisation characteristics was found to be the laser-beam depolarisation. It is important when the depolarised component is comparable with the coherent-scattering component $(S_2^2 + S_3^2)^{1/2}$. This mechanism is most pronounced for the samples with anomalies of radiative characteristics, in the range of the kink in the light–current characteristic. For example, at currents of ~ 225 mA the fraction of the depolarised TM component for sample 2 is almost an order of magnitude larger than that of the coherent component, whereas the coherent component dominates at lower currents. Thus, we found that the kink is accompanied by anomalies in not only the conventional basic characteristics but also in the polarisation characteristic; here, this is a decrease in the degree of polarisation. Obviously, the depolarised TM component is also present at currents beyond the anomaly range; however, in this case, as in the above-considered example, its fraction is much smaller than the coherent-scattering intensity. Since the depolarised TM wave is not completely coherent to the TE wave, the second mechanism is most likely to be due to the presence of dynamic (varying in time and possibly space) optical inhomogeneity with birefringence. The following fact is in favour of this suggestion: in the samples under study the difference in the effective refractive indices for the TE and TM polarisations is such that an optical path difference of about a wavelength arises between these components along the cavity length (~ 1 mm). In addition, different longitudinal modes (whose existence is evidenced by the character of lasing spectrum) can generate corresponding TM waves with different phase shifts, which should also depolarise radiation.

4. Conclusions

The three-band model under study makes it possible to calculate fairly accurately the degree of polarisation of spontaneous emission of InGaAs/AlGaAs and GaAs/AlGaAs lasers with a quantum-well active region. This conclusion, along with the results of [8], confirms the validity of the three-band model for calculating the material

parameters of quantum-well laser active media operating in the spectral range of 0.85 – 0.98 μm.

The degree of polarisation is sensitive to the anomaly (kinks) of laser diodes, which is caused by the deformation of transverse distribution of the laser mode field. In this case, the radiation is depolarised and, correspondingly, the degree of polarisation decreases.

In the regular working regime (beyond the kinks) the presence of the TM component is mainly related not to the radiation depolarisation but to the change in the polarisation state, which is caused by coherent scattering of radiation in the laser cavity. The difference between the laser radiation polarisation from the polarisation of linearly polarised TE radiation can be considered as a characteristic of cavity quality. The geometric sum of the Stokes parameters S_2 and S_3 can be used as a quantitative measure of this difference.

Acknowledgements. This study was supported in part by UNK FIAN. We are grateful to A.E. Drakin for the help in carrying out the experiment.

References

1. Jopson M., Eisenstein G., Hall K.L., Raybon G., Burrus C.A., Koren U. *Electron. Lett*., **22** (21), 1105 (1986).
2. Morito K., Ekawa M., Watanabe T., Kotaki Y. *J. Lightwave Technol*., **21** (1), 176 (2003).
3. Mori Y., Shibata J., Kajiwara T. *Appl. Phys*., **51** (24), 1971 (1987).
4. Kehr A., Muller R., Voss M., Barwolff A. *Appl. Phys. Lett*., **64** (7), 830 (1994).
5. Florescu D.I., Lee D.S., Ting S.M., Rammer J.S., Armour E.A. *J. Electron. Mater*., **32** (11), 1330 (2003).
6. Jayavel P., Kita T., Wada O., Ebe H., Sugawara M., Arakawa Y., Nakata Y., T Akiyama T. *Jpn. J. Appl. Phys*., **44**, 2528 (2005).
7. Matsui Y., Vakhshoori D., Peidong Wang, Peili Chen, Chih-Cheng Lu, Min Jiang, Knopp K., Burroughs K., Tayebati P. *IEEE J. Quantum Electron*., **39** (9), 1037 (2003).
8. Batrak D.V., Bogatova S.A., Borodaenko A.V., Drakin A.E., Bogatov A.P. *Kvantovaya Elektron*., **35** (4), 316 (2005) [*Quantum Electron*., **35** (4), 316 (2005)].
9. Born M., Wolf E. *Principles of Optics: Electromagnetic Theory of Propagation, Interference, and Diffraction of Light* (Oxford: Pergamon, 1964; Moscow: Nauka, 1970).
10. Popovichev V.V., Davydova E.I., Marmalyuk A.A., Simakov A.V., Uspenskii M.B., Chel'nyi A.A., Bogatov A.P., Drakin A.E., Plisyuk S.A., Stratonnikov A.A. *Kvantovaya Elektron*., **32** (12), 1099 (2002) [*Quantum Electron*., **32** (12), 1099 (2002)].
11. Plisyuk S.A., Akimova I.V., Drakin A.E., Borodaenko A.V., Stratonnikov A.A., Popovichev V.V., Bogatov A.P. *Kvantovaya Elektron*., **35** (6), 515 (2005) [*Quantum Electron*., **35** (6), 515 (2005)].
12. Baryshev V.I., Bogatov A.P., Duraev V.P., Eliseev P.G., Luk'yanov S.A., Rakhval'skii M.P. *Kvantovaya Elektron*., **17** (9), 1147 (1990) [*Sov. J. Quantum Electron*., **20** (9), 1057 (1990)].
13. Bogatov A.P., Boltaseva A.E., Drakin A.E., Belkin M.A., Konyaev V.P. *Kvantovaya Elektron*., **30** (4), 315 (2000) [*Quantum Electron*., **30** (4), 315 (2000)].
14. Bogatov A.P., Drakin A.E., Stratonnikov A.A., Konyaev V.P. *Kvantovaya Elektron.,* **30** (5), 401 (2000) [*Quantum Electron*., **30** (5), 401 (2000)].
15. Berry H.G., Gabrielse G., Livingston A.E. *Appl. Opt*., **16** (12), 3200 (1977).
16. Bogatov A.P., Eliseev P.G., Okhotnikov O.T., Pak G.T. *Kvantovaya Elektron*., **7** (8), 1664 (1980) [*Sov. J. Quantum Electron*., **10** (8), 963 (1980)].
17. Eliseev P.G., Okhotnikov O.T., Pak G.T. *Kvantovaya Elektron*., **7** (8), 1670 (1980) [*Sov. J. Quantum Electron*., **10** (8), 966 (1980)].
18. Plisyuk S.A., Batrak D.V., Drakin A.E., Bogatov A.P. *Kvantovaya Elektron*., **36** (11), 1058 (2006) [*Quantum Electron*., **36** (11), 1058 (2006)].
19. Corzine S.W., Yan R.H., Coldren L.A. *Quantum Well Lasers*. Ed. by P.S.Zory (San Diego: Acad. Press Inc., 1993).
20. *Properties of Aluminium Galium Arsenide EMIS Datarewiews Ser. No. 7* (London: INSPEC, 1993).
21. *Properties of Lattice-Matched and Strained Indium Gallium Arsenide EMIS Datareviews Ser. No. 8* (London: INSPEC, 1993).
22. Alaverdyan S.A., Bazhenov V.Yu., Bogatov A.P., Gurov V.Yu., Eliseev P.G., Okhotnikov O.T., Pak G.T., Rakhval'skii M.P., Khairetdinov K.A. *Kvantovaya Elektron*., **7** (1), 123 (1980) [*Sov. J. Quantum Electron*., **10** (1), 68 (1980)].